J Mater Sci (2007) 42:4502–4507
DOI 10.1007/s10853-006-0489-6

Thermal and optical properties of zinc halotellurite glasses

El Sayed Said Yousef

Received: 10 March 2006 / Accepted: 1 June 2006 / Published online: 15 February 2007

Abstract Zinc halotellurite glasses were studied with respect to the glass transition, softening temperature, thermal expansion, optical energy gap, Urbach energy, density, molar volume, refractive index, polarizability, molar refraction and third order non-linear optical susceptibility. Thermal characteristic were determined using a dilatometry. The optical absorption in the wavelength range (300–3200 nm) was measured. From the absorption edge studies, the values of optical band gap (E_{opt}) and Urbach energy (ΔE) have been evaluated. Optical parameters viz., color dispersion, dispersion energy, E_d, average oscillator energy, E_0, and third order non-linear optical susceptibility values are estimated from measuring the refractive index at different wavelength. Results obtained are discussed in terms of the glass structure.

Introduction

Oxyfluoride, oxychloride and oxybromide ions have long been known to be a good glass former and a potential component in optic glasses. Chlorotellurite glasses are interesting because we are able to draw an optical fiber from it that can transmit in the infrared range. Therefore, this glass will have a potential use for building in fiber acousto-optic modulators. Such modulators have the advantage of low insertion loss, high damage threshold, and negligible back reflection. They have applications, for example, in fiber sensors, and in, Q, switching and model locking of fiber lasers [1–3]. The combination of tellurite and halide system has further extended the families of optical glasses. Currently, oxyhlide-tellurite oxide fibers have been studied as rare earth hosts to expand amplification bandwidth for rare earth doped fiber amplifiers as they have low energy phonons and many rare earth ions become optically active in them [4, 5]. Tellurite glasses modified by halides already have been investigated, e.g., $TeO_2/PbF_2/Al_2O_3$, $TeO_2/PbO/PbCl_2$, $TeO_2/PbO/PbBr_2$ and $TeO_2/Li_2O/LiBr$ [6], $TeO_2/ZnO/ZnCl_2$ [7], TeO_2/PbX_2 (X = Br, Cl, F), $TeO_2/PbO/ZnF_2$ [8] and $TeO_2/ZnO/ZnF_2$ glasses [5]. Yousef et al. [9, 10] have investigated binary glasses in the system TeO_2/WO_3 modified by ZnF_2. This paper provides a study on thermal and optical properties of $60TeO_2/40ZnR_2$ mol%, (where, R = F, Cl, Br).

Experimental procedure

Glasses in the $60TeO_2/40ZnR_2$ where (R = F, Cl, Br) system were prepared using a conventional melt quenching method. The powder mixture was given in a gold crucible and heated in a melting furnace under especial temperature program in the range of 400 °C–750 °C, the total time of this melting program equal 4.0 h. The melts were stirred to increase homogeneity. The melt which had a high viscosity was cast at range 500 °C–550 °C in brass mold. Subsequently, the sample was transferred to an annealing furnace and kept for 0.5 h at 210 °C, and 0.5 h at 195 °C and finally 0.5 h at 180 °C. Then the furnace was switched off and the

E. S. S. Yousef (✉)
Physics Department, Faculty of Science, Al-Azhar University, Assiut Branch, Assiut 002, Egypt
e-mail: omn_yousef2000@yahoo.com

glass sample was allowed to cool. The batch weight was 100 gm.

The glasses sample were cut, ground and polished. We made flat sample with parallel surfaces of thickness 1 and 11 mm and prism with dimensions of about 30 mm × 15 mm × 15 mm. Theraml characteristic was defined by a dilatometer on sample with dimensions 20 mm × 5 mm × 5 mm.

The glass transition temperature, (T_g), transformation temperatures of glass sample near the eutectic composition, (softening temperature, T_s), and linear thermal expansion, (α_t), were measured, using pushrod a dilatometer (Dilatometer Netzsch 402 E) at a heating rate 5 K/min.

The UV transmittance of the glasses was determined at wavelengths from 200 nm to 3,200 nm with an error of <1%, using a Shimadzu 3101PC spectrophotometer with optical pathlengths of 1 mm and 11 mm (i.e., sample thickness of 10 mm).

From the glass samples, prisms of dimensions 30 mm × 15 mm × 15 mm were cut. The refractive indices of the prepared sample were measured using a prism spectrometer, at the wavelengths 643.8 nm (C\-line from cadmium spectrum), 546.1 nm (e-line from hydrogen spectrum), 479.98 nm (F\-line from cadmium spectrum) and 435.8 nm (g-line from hydrogen spectrum). The error was $\Delta n \pm 5 \times 10^{-5}$.

Results and discussion

Table 1 shows T_g (in °C), T_s (in °C), $\Delta T = T_s - T_g$ (in °C) and thermal expansion, α_t, ($\times 10^{-7}$/K). The value of glass transition of present glass lies in the range 225 °C–247 °C. The glass transition temperature, T_g, increase in the series $ZnF_2 < ZnCl_2 < ZnBr_2$ direction. The atomic weight, atomic ring size of network, number of immediate neighbors, number of bridging bonds, force constant determine the density and the glass transition temperature. However, the increase in T_g usually means a closer network but the decrease in glass transition temperature means a more open network of the prepared glasses [5]. Many authors reports that, when add halide ion to tellurite glasses occur gradual reduction of the tellurium coordination state from 4 → 3 [11, 12]. In the prepared glass, replacement of TeO_2 by ZnR_2 (R = F, Cl, Br) due to the increase of the rigidity of the glass network in the direction ($ZnF_2 \rightarrow ZnCl_2 \rightarrow ZnBr_2$). And also, the addition of ZnR_2 (R = F, Cl, Br) to the TeO_2 glass decrease the concentration of Te–O bonds; moreover, halide ions can come into TeO_4 network by replacing O^{2-} and open Te–O–Te bridge oxygen bond, which decrease the rigidity of TeO_4 network.

It should be noted that, ZnF_2, $ZnCl_2$ or $ZnBr_2$ causes splitting of O–Te–O bonds. It would also, ZnF_2 into glass interstices, more and more ions being open up in the network. Therefore, the weakening of the glass structure or reduction in the rigidity of the network take place is higher at composition $60TeO_2/40ZnF_2$ glass.

It has been confirmed that, the ratio between TeO_3/TeO_4 of the studied sample are in following the order $60TeO_2/40ZnF_2 > 60TeO_2/40ZnCl_2 > 60TeO_2/40ZnBr_2$.

The value of thermal stability, $\Delta T = T_s - T_g$ (in °C), were used in the fiber draw. It is obvious that, ΔT, increase in the direction $ZnF_2 \rightarrow ZnCl_2 \rightarrow ZnBr_2$. O'Donnell et al. [13] expected as fluoride tends break up the strong TeO_2 covalent network of the glass by forming ionic non-bridging M–F bonds (where M is a cation) enabling the glass-forming liquid to flow more easily at lower temperature; hence viscous points occur at lower temperature. This leads to; the smallest value of ΔT obtained in the glass with the composition $60TeO_2/40ZnF_2$ (see Table 2)

The linear thermal expansion coefficient is defined as, $\alpha_t = (1/L_0)(\Delta L/\Delta T)$, where L_0 is the length of sample before heating, it corresponds to the respective slope of L (T) curve normalized to the value at the transition temperature. The values of linear thermal expansion of the prepared glass are between 187 and $207 \times 10^{-7}/K^{-1}$. It decreases in the order $ZnF_2 \rightarrow ZnCl_2 \rightarrow ZnBr_2$ in the glass matrix. The bond strengths of halide ions are, Zn–F = 67 ± 2.8 kcal/mol^{-1}, Zn–Cl = 54.4 ± 4.7 kcal/mol^{-1}, Zn–Br = 34 ± 7 kcal mol^{-1} [14]. We can suggest that in the present glass the linear thermal expansion increase

Table 1 Glass transition, softening temperature, thermal expansion, Urbach energy and optical energy of the prepared glasses

System composition, in mol%		Glass transition, T_g in °C	Soft temperature, T_s (in °C)	ΔT, ($T_g - T_s$) (in °C)	Error, ±°C	Thermal expansion, α_t (10^{-7}/K)	Error, ±K	Urbach energy, E_e (in eV)	Optical energy, E_{opt} (in eV)
$60TeO_2$	$40ZnF_2$	220	250	30	±5	207	±5	0.059	3.11
$60TeO_2$	$40ZnCl_2$	230	262	32	±5	199	±5	0.06	3.08
$60TeO_2$	$40ZnBr_2$	247	283	36	±5	187	±5	0.057	3.05

Table 2 Compositions, densities, molar volumes, refractive indices at different wavelengths and relative dispersion of the prepared glasses

System composition, in mol%		Density, (in g cm^{-3})	Molar volume, (in cm^3)	Refractive index				Error, $\pm\Delta n$	Relative dispersion, $\frac{n_g - n_{F\backslash}}{n_{F\backslash} - n_{C\backslash}}$
				$C\backslash$ (643.8 nm)	E (546.1 nm)	$F\backslash$ (479.98 nm)	g (435.8 nm)		
$60TeO_2$	$40ZnF_2$	4.2828	32.02	1.9164	1.9373	1.9612	1.9859	±0.0005	0.551
$60TeO_2$	$40ZnCl_2$	4.3675	34.41	1.9275	1.9486	1.9728	1.9976	±0.0005	0.547
$60TeO_2$	$40ZnBr_2$	4.4372	41.8	1.9382	1.9594	1.987	2.016	±0.0005	0.594

with increasing both non-bridging oxygen and the bond strengths of halide ions in the glass matrix. Also, El-Mallawany [1] reported that, the weakening of the glass network with halide ions substitution due to the decrease in elastic modulus.

The interatomic distance of halides is (Zn–F = 1.81 Å, Zn–Cl = 2.05 Å, Zn–Br = 2.21 Å) [15]. The atomic weight of halide ions changes from lower to higher in the direction ($ZnF_2 \rightarrow ZnCl_2 \rightarrow ZnBr_2$). This increase in the density with ZnR_2 (where R = F, Cl and Br) related to the change in the atomic weight and interatomic distance. Change of molar volume also in the same direction (see Table 2).

UV, VIS and NIR transmission spectra of prepared glasses are shown in Fig 1a. The absorption in the UV and VIS spectral ranges is caused by electron transitions from unexcited to excited states. The present glasses have a better UV transmission (see Fig. 1a). Stevels [16] described the dependence of the UV transmission on the content of the network modifiers

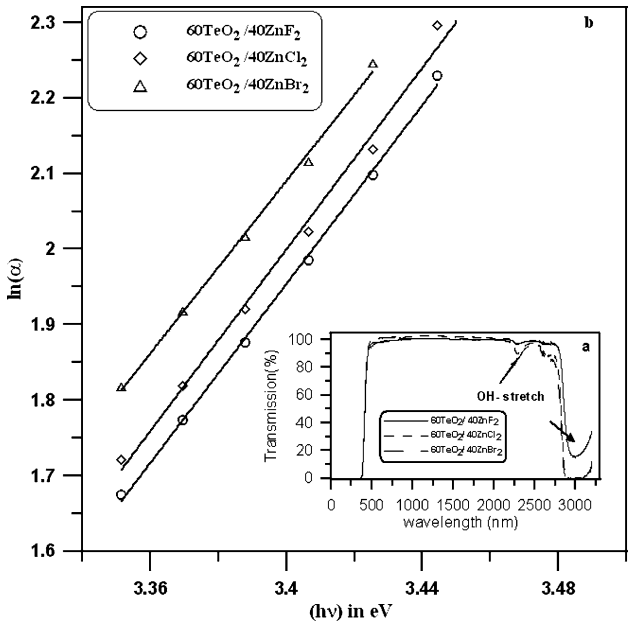

Fig. 1 (**a**) UV, VIS and NIR transmission spectra of the prepared glasses (sample thickness of 10 mm). (**b**) ln(α) as a function of , hν, of the prepared glasses

and the non-bridging oxygens. When the transfer of an electron located at the anion (F, Cl, Br) to an unoccupied energy gap of a ligand cation is easier lead to the more easily oxidized of the ligand [17]. Therefore, the absorption in crystalline compounds shifts in the series fluorides → chlorides → bromides from the UV spectral region to longer wavelengths in the VIS region. The absorption bands were appeared near to 3.2 μm–4.4 μm due to OH^--stretching vibrations of the free OH groups in the prepared glasses (see Fig. 1a).

The optical absorption coefficient, ($\alpha\nu$), in the optical region near the band edge in many amorphous semiconductor shows an exponential dependence on the photon energy, $h\nu$, and obeys an empirical relation due to Urbach [18],

$$\alpha(\nu) = \alpha_0 \exp(h\nu/E_e) \quad (1)$$

where, ν is the frequency of radiation, α_0 is a constant, and, E_e is related to the width of the tail of localized states in the band gap. The physical origin of, E_e, can be attributed to the phonon-assisted indirect electronic transitions. Tauc [19] reported that, the exponential variation of, α, with, $h\nu$, is due to transitions between localized states and will vary from sample to sample where as Davis and Mott [20] assumed that the value of E_e will be much the same for most amorphous semiconductors. In the present work, the values of Urbach energy calculated by taking the reciprocals of slopes of the linear portion of the ln $\alpha(\nu)$ versus hν curves in the lower photon energy regions (see Fig. 1b). The values of, E_e, are listed in the Table 1 for all samples. The value of, E_e, lie between 0.057 eV and 0.061 eV in the prepared glasses and the minimum value recoded at composition $60TeO_2/40ZnBr_2$ indicate that these glasses are highly homogeneity. Mott and Davis [20] relate this data to the optical band gap, E_{opt}, through the following general relation proposed for amorphous materials;

$$\alpha(\nu) = \frac{B(h\nu - E_{opt})^r}{h\nu} \quad (2)$$

where the index, r, takes different values depending on the mechanism of interband transition, B is a constant and, hν, is the photon energy of incident photon. Equation (1) depicts a straight line for $r = 2$ and is associated with indirect allowed transitions in most glasses. Figure 2 represents the Tauc's plot $(\alpha h\nu)^{1/2}$ versus (hν) for different samples. The E_{opt} has been estimated from the linear regions of the curves by extrapolating them to meet the, hν, axis at $(\alpha h\nu)^{1/2} = 0$ and the values are listed in Table 1 for all the samples. The value of the optical energy gap in the range 3.05 eV–3.11 eV obtained in prepared glasses (see Table 1). Moreover, the results seem to increase in a systematic manner in the order $60TeO_2$–$40ZnF_2$ > $60TeO_2$–$40ZnCl_2$ > $60TeO_2$–$40ZnBr_2$. McSwain et al. [21] suggested that the shift from higher to lower energies or a change in the absorption band characteristics related to a transition to non-bridging oxygens, which bind excited electrons less tightly than bridging oxygen's. Therefore, the optical energy gap of the present glasses in Table 1 is in a good agreement with this dependence.

Sahar et al. [7] reported that the value of optical energy gap in TeO_2/ZnO/$ZnCl_2$ in the range 2.0 eV–2.5 eV could provide some encouragement for further study, especially for a longer wavelength application. The present glass have largest value of optical energy gap provides a possibility that this glass may applicable in the optical devices components.

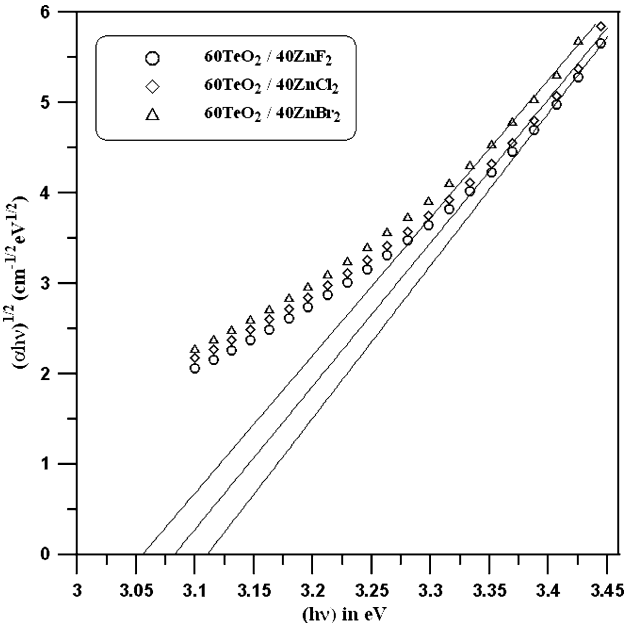

Fig. 2 $(\alpha h\nu)^{1/2}$ as a function of, hν, of the prepared glasses

The refractive index, n, depends on number of electrons and polarization. The values of refractive index increase in the $ZnF_2 \rightarrow ZnCl_2 \rightarrow ZnBr_2$ direction (see Table 2). We know that, the non-bridging oxygen NBO bonds have a much greater ionic character and much lower bond energies. The electronic polarizability, α_e, (in Å^3) for F^- = 1.04, Cl^- = 3.66 and Br^- = 4.77 [17].

This qualitatively explains the present data, the glass $60TeO_2/40ZnF_2$ has a smallest value of refractive index, the smallest electronic polarizability and highest non-bridging oxygen. The glass in the composition $60TeO_2/40ZnBr_2$ has a highest refractive index, the largest value of electronic polarizability and lowest NBO. The relative depressive power of the prepared glasses defined as $[n_g - n_F]/[n_F - n_C]$, where n_C, n_F and n_g are the refractive indices at the wavelength C = 643.8 nm, F = 479.98 nm, and g = 435.8 nm, respectively.

The value of relative depressive power is in opposite trend with Urbach energy (see Tables 1, 2). This means that, the sample has highest value of Urbach energy, the lowest value of relative dispersion energy, and smallest disorder in the amorphous structure.

The molar refractivity, R_m, calculated by using the relationship [22];

$$R_m = \left(\frac{n_0^2 - 1}{n_0^2 + 2}\right) V_m \tag{3}$$

where, n_0 is the refractive index and, V_m is molar volume (in m^{-3}) obtained from density and the average molecular weight. The value of molar refraction increases from to 15.09 to 20.02 (in cm^3 mol^{-1}), when zinc halide change in the direction $ZnF_2 \rightarrow ZnCl_2 \rightarrow ZnBr_2$ (see Table 2). The molar refraction of the TeO_2/M_2O glass depends upon the ionic refraction of the modifier (M). The ionic refraction in crystal compounds depends upon at these factors; (i) the electronic polarizability of the ion, which increases as the number of electrons of in the ion increases, (ii) the coordination number of the ion, (iii) the polarizability of the first neighbor ions coordinated with it. The value of molar refraction of the present glass is in a good accord with this dependence.

The polarizability of the glass, α_m, is proportional to molar refraction and it determine by the relation as follow [23];

$$\alpha_m = \frac{3}{4\Pi N} \cdot \frac{n^2 - 1}{n^2 + 2} \cdot V_m \tag{4}$$

where N is Avogadro's number. The electronic polarizability increases in the direction $F^- \rightarrow Cl^- \rightarrow Br^-$. This lead to the polarizability of the studied sample is in following the order $60TeO_2/40ZnF_2 < 60TeO_2/40ZnCl_2 < 60TeO_2/40ZnBr_2$ from 5.99 Å^3 to 7.9 Å^3 (see Table 2).

The relation between the refractive index and photon energy shown in Fig. 3 gives us very important information concerning the energy state of electrons as indicated by Wemple. He derived the dependence of refractive index on photon energy by assuming the single-oscillator approximation on the basis of the Kramers-Kronig relation as follows [24];

$$\frac{1}{n^2-1} = \frac{E_s}{E_d} - \frac{E^2}{E_s E_d} \tag{5}$$

where, n is the refractive index at a specific wavelength, E_s is the average excitation energy for electronic transitions and E_d represents the electronic oscillator strength relation dispersion. E_s and E_d values were calculated in terms of the linear fit of $1/(n^2 - 1)$ versus E^2 (see Fig. 3). The value of E_s lies in the range 7.19–6.9 (in eV) and E_d lies in the range 17.53–18.15 (in eV). Almost of previously studied glasses [23], which have larger values of refractive index, were related to smaller values of E_s and E_d. This relation is in a good agreement with the present halotellurite systems were studied (see Table 2).

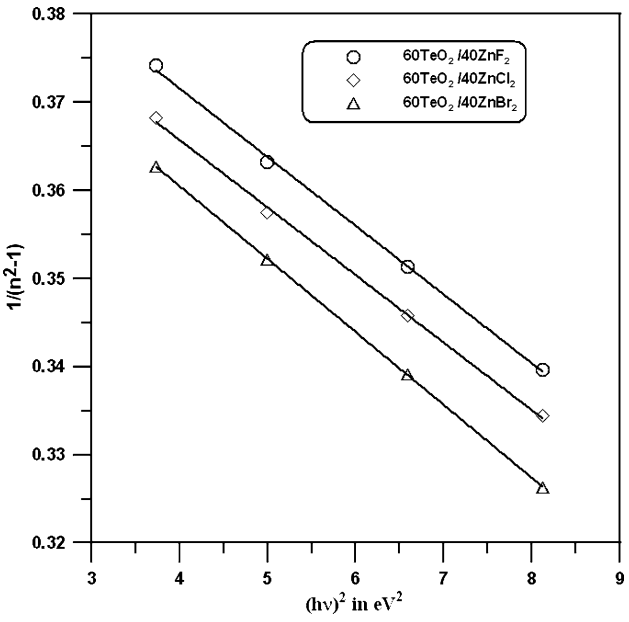

Fig. 3 The dependency of the refractive indices as a function of the photon energy (illustrated as $1/(n^2–1)$ versus E^2)

Lines [25] estimated the third order non-linear susceptibilities $\chi^{(3)}$ of a large number of ionic and covalent monoxides, which gives by the formula;

$$\left(\frac{\chi^{(3)}}{d^2}\right) = \frac{0.26 \times 10^{-12} f_l^3 (n_w^2 - 1) \cdot E_s^6}{(E_s^2 - E^2)^4} \text{ esu/Å}^2 \tag{6}$$

where, f_l, is the Lorentz field factor $[(n_w^2 + 2)/3]$, n_w is the refractive index at wavelength, w, E_s is the Sellmeier gap, E the photonenergy (hν) and, d, the M–O bond length in Å. As it difficult to evaluate the bond length, d, for prepared glasses, only the values of $(\chi^{(3)}/d^2)$ was calculated. The value of $(\chi^{(3)}/d^2)$ is in the range from 0.95 to 1.12×10^{-13} (in esu/ Å^2).

The smallest value of third order non-linear susceptibilities was obtained in the glass with the composition $60TeO_2/40ZnF_2$. In other hand, the largest of third order non-linear susceptibilities were obtained in the glass with the composition $60TeO_2/40ZnBr_2$ (see Table 3).

This phenonemena are explainable as follows; TeO_2 replaced by zinc halide due to a structural variation from $TeO_4^{4-} \rightarrow TeO_3^{2-}$ entities through an intermediate asymmetric structure. This deformation causes a decrease in the non-bridging oxygens (NBO) in the $60TeO_2/40ZnF_2 \rightarrow 60TeO_2/40ZnCl_2 \rightarrow 06TeO_2/40ZnBr_2$ and is therefore responsible for high linear and non-linear indices. However, the charge density of O^{2-}, F^-, Cl^- and Br^- decreases in that order $O^{2-} \rightarrow F^- \rightarrow Cl^- \rightarrow Br^-$ ions donate fewer electrons to Te through $Te–Cl_{eq}$, $Te–F_{eq}$ and $Te–Br_{eq}$ bond, respectively. Consequently, the electron transfer from Te to O in the $Te–O_{ax}$ bond is smaller, and therefore, the degree of the weakening of the $Te–O_{ax}$ bond, which brings about the formation of TeO_3^{2-}, is smaller when F^-, Cl^- and Br^- ions occupy the equatorial position than when an O^{2-} ion does [26]. In other words: the $Te–O_{ax}$ bond is stronger when Br^- ion occupies the equatorial position that when F^- and Cl^- ion does, leading to higher wavenumber of the $Te–_{ax}$ stretching vibration. The value of anion electronegativities for halide ions is following; (F = 4.0, Cl = 3.0, Br = 2.8), respectively. This explains the present data; the glass $60TeO_2/40ZnBr_2$ has highest value of third order non-linear susceptibility but the glass $60TeO_2/40ZnF_2$ has smallest value of third order non-linear susceptibility.

The relationship between $(\chi^{(3)}/d^2)$ and E_d/E_s^2 in Eq. (6) indicating that the value of $\chi^{(3)}$ increased almost linearly with increasing E_d/E_s^2. This implies that small average excitation energy and a large dispersion yield a high $\chi^{(3)}$ value. Here, this relation is valid in the present glasses as shown in Fig. 4.

Table 3 Molar refraction, polarizability, dispersion energy (in eV), oscillator energy (in eV) and third order non-linear susceptibility of the prepared glasses

System composition, in mol%		Molar refraction, R_m (in cm^3 mol^{-1})	Polarizability, α_m (in $Å^3$)	Dispersion energy, E_d (in eV)	Osillator energy, E_s (in eV)	Third order non-linear susceptibility, $(x^{(3)}/d^2)$ in 10^{-13} esu/$Å^2$
$60TeO_2$	$40ZnF_2$	15.09	5.99	17.85	7.19	0.95
$60TeO_2$	$40ZnCl_2$	16.35	6.5	18.15	7.19	0.99
$60TeO_2$	$40ZnBr_2$	20.02	7.9	17.53	6.9	1.12

Conclusion

Optical properties, density, linear thermal expansion, transmittance in the UV–VIS and NIR of the glasses show the zinc halotellurite glasses are flint type with good spectral transmittance. Introduction of zinc halide in the direction $ZnF_2 \rightarrow ZnCl_2 \rightarrow ZnBr_2$ into the tellurite matrix increases the glass transition temperature, refractive index and third order non-linear susceptibility. The thermal expansion coefficient, optical energy and oscillator energy of the present glasses are in the series $60TeO_2/40ZnF_2 > 60TeO_2/40ZnCl_2 > 60TeO_2/40ZnBr_2$. This explained by, transformation from a rigid formula character of TeO_4 to a matrix of regular TeO_3 units, which results in loose packing of the glass network. Large values of E_{opt} in the range of 3.05 eV–3.11 eV in the present glasses could provide some encouragement for further study, especially for longer wavelength application.

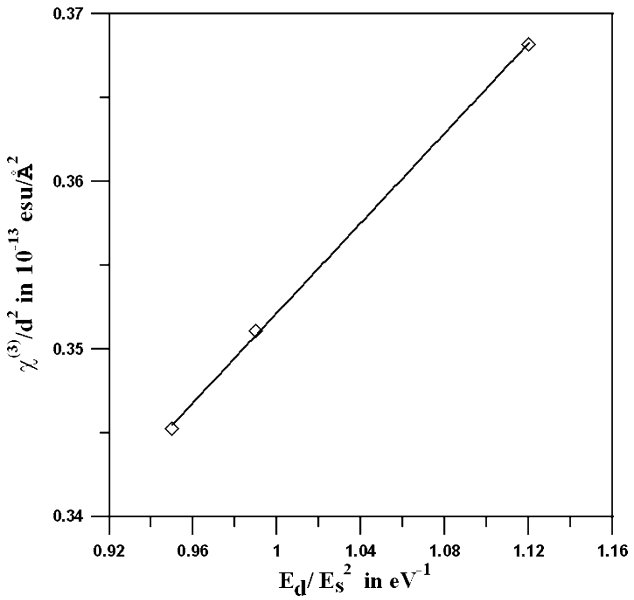

Fig. 4 The dependency of the third order optical susceptibility as a function of the E_d/E_s^2 [illustrated as $(\chi^{(3)}/d^2)$ versus (E_d/E_s^2)]

References

1. El Mallawany RAH (2001) Tellurite glasses handbook—physical properties and data. CRC, Boca Raton, FL
2. Abdulhalim I, Pannel CN, Wang J, Wylangoweski G, Payne DN (1994) J Appl Phys 75(1):519
3. J. Wang (1993) Novel multicomponent glasses and fibres for fibre-optic devices and systems, Ph.D. thesis, University of Southampton, March
4. Zhu D, Zhou W, Zhao H (2001) J Non Cryst Solids 281:86
5. Nazabal V, Todoroki S, Inoue S, Matsumoto T, Suehara S, Hondo T, Araki T, Cardinal T (2003) J Non Cryst Solids 326&327:359
6. Kozhukharov V, Burger H, Neov S (1991) Mater Sci Forum 67&68:143
7. Sahar MS, Noordin N (1995) J Non-Cryst Solids 184:137
8. Liu YH, Chen DD, Zhang QY, Jiang ZH (2006) Optical Mater 28(4):302
9. Yousef E, Hotzel M, Russel C (2004) J Non-Cryst Solids 342:82
10. Yousef El Sayed (2005) J Phys D Appl Phys 38:3970
11. Wang Guonian, Zhang Junjie, Dai Shixun, Wen Lei, Yang Jianhu, Jiang Zhonghong (2005) J Molecular Struct 750:1
12. Hoppe U, Yousef E, Russel C, Neuefeind J, Hannon AC (2002) Solid State Commun 123:273
13. O'Donnell MD, Miller CA, Furniss D, Tikhomirov VK, Seddon AB (2003) J Non Cryst Solids 331:48
14. R. Weast (ed) (1980 &1981) Handbook of Chemistry and Physics, 61st edn. CRC Press, Boca Raton, Florida, p. F223
15. Krasnov K, Philipenko H, Bobkova V (1979) Molecular constants of the inorganic compounds. Khimia, Leningrad, p 46
16. Stevels J (1948) Verres Refract 2:2
17. Burger H, Vogel W, Kozhukharov V (1985) J Infrared Pys 25:395
18. Urbach F (1953) Phys Rev 92:1324
19. J. Tauc (1970) In: Abeles (ed) The optical properties of solids. North Holland, Amsterdam, p 227
20. Davis EA, Mott NF (1970) Phil Mag 22:903
21. McSwain BD, Borrelli NF, Su G-J (1963) Physics Chem Glasses 4(1):1
22. Reddy R, Nazeer Ahmed Y, Abdul Azeem P, Rama Gopal k, Rao TVR (2001) J Non-Cryst Solids 286:169
23. Kim Sae Hoon, Yoko Toshinobu, Sakka Sumio (1993) J Am Ceram Soc 76(4):865
24. Wample SH (1977) J Chem Phys 67:2151
25. Lines ME (1991) Phys Rev B 41:3372
26. Tanaka K, Yoko T, Yamada H, Kamiya K (1988) J Non Cryts Solids 103:250